

A new approach on human–robot collaboration with humanoid robot RH-2

C. A. Monje^{†*}, P. Pierro and C. Balaguer

Department of Systems Engineering and Automatics, University Carlos III of Madrid, Madrid, 28911/Leganés, Spain

(Received in Final Form: February 16, 2011. First published online: March 18, 2011)

SUMMARY

This paper presents a novel control architecture for humanoid robot RH-2. The main objective is that a robot can perform different tasks in collaboration with humans in working environments. In order to achieve this goal, two control loops have to be defined. The outer loop, called collaborative control loop, is devoted to the generation of stable motion patterns for a robot, given a specific manipulation task. The inner loop, called posture stability control loop, acts to guarantee the stability of humanoid for different poses determined by motion patterns. A case study is presented in order to show the effectiveness of the proposed control architecture.

KEYWORDS: Humanoid robot RH-2; Human–robot collaboration; Control architecture; Kinematic model; Dynamic model.

1. Introduction

In real life, the use of robots in typical human environments could be really profitable, especially in tasks that robots can perform in collaboration with human beings. When robots have to collaborate with humans, their interaction capabilities become really important, even if not sufficient.

Many research efforts have been concentrated on modalities of the interaction between these two agents (i.e. dialogue, joint solution of problems, etc).¹ A human can interact with a robot using different tools, such as a Personal Digital Assistant (PDA) system or a joystick.² A coordinated task between a human and a mobile manipulator has been analyzed by Yamamoto *et al.*,³ where the mobile manipulator follows the trajectory while executing a task together with a human. Of course, the main issue in the human–robot physical interaction is the whole-body control problem under several constraints and obstacles, already extensively presented in literature.^{4,5}

The human–robot collaboration has a common framework with respect to human–robot interaction: It is important that the robot partner perceives human intentions or goals in order to achieve a common objective.⁶ In order to reason human

intentions during a collaborative task (such as collaborative transportation or assembly), sensorial system of a robot should be integrated. Information coming from this system becomes an input to the control algorithm, which allows to carry out the collaborative task or joint manipulation while maintaining the whole system stable. First of all, stable motion patterns must be generated from the information of the sensorial system. Then a pose control is needed to guarantee the stability of humanoid for different poses determined by motion patterns.

For the generation of stable motion patterns, the Generalized Inverted Kinematics (GIK) introduced by Nakamura *et al.*⁷ to control redundant robots is widely used in humanoid robotics,^{8,9} as well as its counterpart in the force domain, the Operational Space approach.¹⁰ Based on the notion of task,¹¹ priority between tasks is introduced by projecting the tasks with lower priority in the kernel of tasks having a higher priority. The work by Nakamura *et al.*⁷ has been extended by Siciliano *et al.*¹² to an iterative scheme that allows the determination of joint angles of robot for the execution of a task while accomplishing one or several lower priority subtasks.

In this paper, and based on Siciliano *et al.*'s¹³ approach, we present a solution to a human–robot collaboration case like the one shown in Fig. 1.

The control architecture proposed has been tested using the model of humanoid robot RH-2. This robot, currently in designing process, is an advanced version of RH-1 (Fig. 2), a prototype totally developed by the research team Robotics Lab in the University Carlos III of Madrid, Spain.

One of the main improvements to RH-2 with respect to its predecessor is the design of ankle. Ankle is fundamental when dealing with walking actions and stability. A picture of ankle's first prototype is shown in Fig. 3. The whole structure acts as an inverted pendulum with a tip mass concentrated at robot's center of mass (COM).

Humanoid gait is often modeled with various versions of inverted pendulum, such as 2D and 3D linear inverted pendulums (LIP),^{14,15} the cart-table model,¹⁶ the variable impedance LIP,¹⁷ the spring-loaded inverted pendulum,¹⁸ and the angular momentum pendulum model (AMPM).^{19,20} These reduced biped models have been very beneficial in the analysis and control of human and humanoid gait. The inverted pendulum models allow us to ignore movements of individual limbs of a humanoid and instead focus on one point of fundamental importance: robot's COM. The model of inverted pendulum used in this work is discussed later.

* Corresponding author. E-mail: cmonje@ing.uc3m.es

† This paper was originally submitted under the auspices of the CLAWAR Association. It is an extension of work presented at CLAWAR 2009: The 12th International Conference on Climbing and Walking Robots and the Support Technologies for Mobile Machines, Istanbul, Turkey.



Fig. 1. Example of a human and a robot jointly transporting a table.



Fig. 2. Humanoid robot RH-1.



Fig. 3. Fist prototype of RH-2 ankle.

The paper is organized as follows. Section 2 shows the proposed global control architecture, including both collaborative (joint manipulation) and posture stability control loops. Section 3 deals with the collaborative control scheme, proposing a kinematic model of arms and a joint manipulation scheme. A case study with simulation results

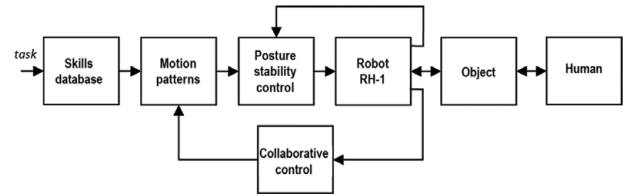


Fig. 4. General control architecture.

is also presented in this section. The posture stability control is aimed in Section 4, using a simplified model of RH-2 dynamics based on single inverted pendulum. Simulation results are also given. Finally, some conclusions and future works are drawn in Section 5.

2. Control Architecture for RH-2

The novel control scheme proposed in this paper is the one shown in Fig. 4, where two different control loops are considered: (a) collaborative control loop, and (b) posture stability control loop.

Given a task, there are different patterns for arms and legs in order to generate a stable pose for robot. The main function of the collaborative control loop is to ensure that these motion patterns are stable and achievable by the robot during joint manipulation. The kinematic model of the robot is needed for that purpose. In an inner loop, a posture control is needed to guarantee stability of a humanoid for different postures determined by motion patterns. In this case, a dynamic model of a robot must be used. The posture must be controlled in real-time through information from encoders of servomotors, since the forces caused by object and man during the activity may undermine system's stability.

Several models can be used in order to achieve stability. Some of these are based on the measurement of Zero Moment Point (ZMP), a point with respect to which the dynamic reaction force at the contact of foot with ground does not produce any moment, i.e., a point where total inertia force is equal to 0. For instance, it is possible to evaluate ZMP and correct the pose online using the force/torque sensors present in the feet. Possible ways of correcting the pose are the compensation of waist position and adjustment of leg joints. Eventually, it is also possible to regulate the position of feet (in case of rough terrain or inevitable errors in the position of feet) and gait velocity.^{21,22}

The ZMP measurement is also important for the quasi online estimation of ZMP evolution. If master's intentions are known in advance, a correct pattern can be chosen for arms and legs. Therefore, using, for instance, space and time prediction, it is possible to calculate the next probable ZMP position in order to select a better walking pattern. A possible approach, proposed in ref. [23], is based on an active human-robot cooperation system based on intention recognition, using the hidden Markov model. However, these solutions come into great algorithm complexities, which makes their use very difficult in real situations.

In this paper, the research is focused on collaborative and posture loops.

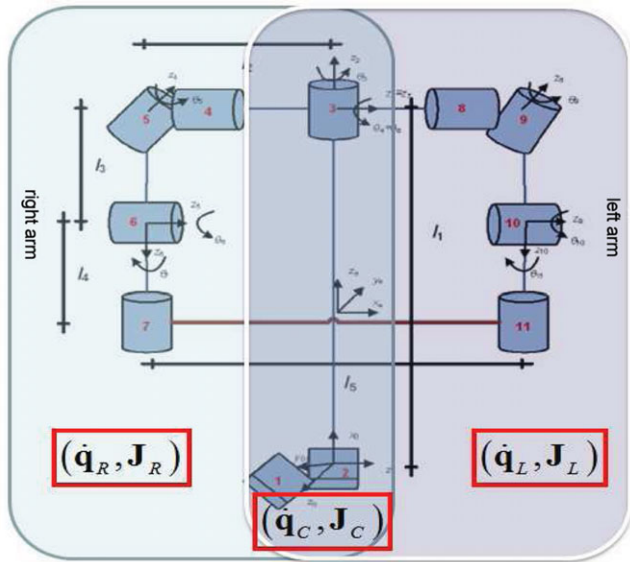


Fig. 5. Kinematic model of the arms.

3. Collaborative Control Loop

In this section, a solution is given for the problem of achieving a joint transportation of an object between a human and a robot.

In this line, Khatib *et al.*⁴ proposed a solution using a task-oriented framework for whole-robot dynamic coordination and control. However, in order to simplify the computational complexity of this algorithm, we propose to study the joint transportation by modeling robot arms and object to be transported as a closed chain. A kinematic model of RH-2 robot has been derived giving the possibility of moving two arms according to a desired trajectory.

3.1. Model of robot arms

While for open-chain manipulators the classical problem is to calculate joint angles and velocities for a given trajectory for an end-effector, in closed-chain manipulators the solution must be calculated considering as a main constraint that the object to manipulate must be supported.

In fact, as shown in Fig. 5, which represents the arms of humanoid robot RH-2 in a schematic way, the closed chain has been cut in the middle of the bar, which becomes the end-effector. The whole kinematics will be solved by calculating each arm's kinematics and imposing the following conditions for a common end-effector:

- Same position with respect to the origin.
- Same orientation with respect to the origin.

The RH-2 arms present several limitations related to robot mechanics.^{2,24} Each arm has only four joints and two arms share a common neck joint. The idea behind this work is to add two virtual prismatic joints. These two joints resume the kinematics of robot legs in such a way that they become a reference for COM.

3.2. Locomotion and manipulation coordination

The concept of "task priority" was introduced by Nakamura *et al.*²⁵ This concept applies to redundant robot manipulators,

where the inverse kinematic problem has to be solved. In fact, by using pseudo-inverse of the Jacobian matrix, it is possible to determine joint angles of a robot for the execution of a task, while accomplishing one or several lower-priority subtasks.¹³

In a previous work,^{2,24} we have demonstrated the possibility of using such a tool in order to find a solution of RH-2 arms in a closed kinematic chain. However, using this solution it is not possible to specify the desired orientation to be followed. The drawback of such a model is that only structure of humanoid arms is considered in the problem of joint manipulation.

The RH-2 arms present 9-degree-of-freedom (DOF), which would not be sufficient for specifying 12-DOF required for carrying out the chain and specifying position and orientation of the end-effector. Here the use of virtual joints will permit to specify the desired trajectory and orientation for a closed kinematic chain associated to humanoid arms. The two virtual prismatic joints resume the kinematics of robot legs. By using simple transformation techniques, it is possible to use the solution of inverse kinematics as a reference to mobile legged part.

Being \mathbf{x}_r and \mathbf{x}_l the position and orientation of right and left arms, respectively, the solutions \mathbf{q}_r and \mathbf{q}_l referring to joint angles must be found.

The tasks to be implemented are as follows:

- Task 1: The end-effector of right and left arms should coincide in position and orientation.
- Task 2: The end-effector must follow the desired trajectory.

The first task can be written as

$$\dot{\mathbf{x}}_r = \dot{\mathbf{x}}_l \Rightarrow \mathbf{J}_r \dot{\mathbf{q}}_r = \mathbf{J}_l \dot{\mathbf{q}}_l, \tag{1}$$

where \mathbf{J}_r and \mathbf{J}_l are the Jacobian matrices of right and left arms, respectively, and $\dot{\mathbf{q}}_r$ and $\dot{\mathbf{q}}_l$ are joint velocities.

Now consider that each arm is constituted of a part that is shared with another arm (i.e., COM of virtual joints and neck joint) and a distinctive part. Denoting the common part as $\dot{\mathbf{q}}_C$ and the distinctive parts of each arm as $\dot{\mathbf{q}}_R$ and $\dot{\mathbf{q}}_L$, it is possible to rewrite Eq. (1) as

$$\begin{aligned} \dot{\mathbf{x}}_r &= \mathbf{J}_r \dot{\mathbf{q}}_r = \mathbf{J}_C \dot{\mathbf{q}}_C + \mathbf{J}_R \dot{\mathbf{q}}_R, \\ \dot{\mathbf{x}}_l &= \mathbf{J}_l \dot{\mathbf{q}}_l = \mathbf{J}_C \dot{\mathbf{q}}_C + \mathbf{J}_L \dot{\mathbf{q}}_L, \end{aligned} \tag{2}$$

where \mathbf{J}_C is a 6×3 matrix, and \mathbf{J}_R and \mathbf{J}_L are two 6×4 matrices related to common and distinctive parts, respectively.

It is possible to write the objectives in the following way:

- Task 1: $\dot{\mathbf{e}}_1 = \mathbf{0} = \mathbf{J}_R \dot{\mathbf{q}}_R - \mathbf{J}_L \dot{\mathbf{q}}_L$.
- Task 2: $\dot{\mathbf{e}}_2 = \dot{\mathbf{x}}_r = \mathbf{J}_C \dot{\mathbf{q}}_C + \mathbf{J}_R \dot{\mathbf{q}}_R$.

Writing the tasks in a conventional way, that is,

$$\dot{\mathbf{e}} = \mathbf{J} \dot{\mathbf{q}}, \tag{3}$$

Equation (3) can be written in a matrix form as follows:

$$\begin{bmatrix} \dot{\mathbf{e}}_1 \\ \dot{\mathbf{e}}_2 \end{bmatrix} = \begin{bmatrix} \mathbf{0} & \mathbf{J}_R - \mathbf{J}_L \\ \mathbf{J}_C \mathbf{J}_R & \mathbf{0} \end{bmatrix} \begin{bmatrix} \dot{\mathbf{q}}_C \\ \dot{\mathbf{q}}_R \\ \dot{\mathbf{q}}_L \end{bmatrix}. \tag{4}$$

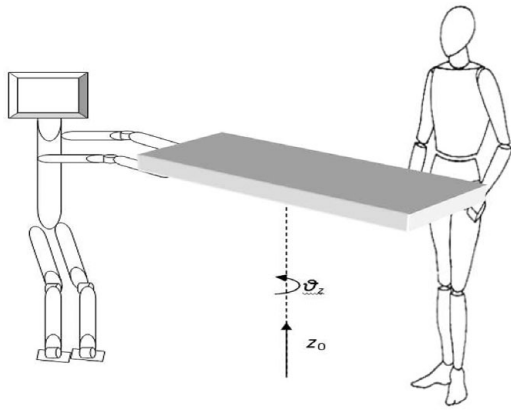


Fig. 6. Case study.

In the most general case, matrix \mathbf{J} in Eq. (3) is composed by two 6×11 matrices. This means that under this assumption and using 6-DOF for the closed kinematic chain, it is possible to specify the end-effector's position and two orientations.

3.3. Case study

When the task to be achieved is a joint transportation, the following assumption can be done: The robot and human will move in the same horizontal plane parallel to ground at height z . In such conditions, only the orientation along z_0 -axis needs to be specified for the end effector, together with the position in three directions. Such a situation is shown in Fig. 6.

Under these assumptions, the Jacobian \mathbf{J} turns into a 10×11 matrix:

$$\dot{\mathbf{q}} = \mathbf{J}^\dagger \dot{\mathbf{e}} = \mathbf{J}^\dagger \begin{bmatrix} \mathbf{0} \\ \dot{\mathbf{p}}_d \\ \omega_{z,d} \end{bmatrix}, \tag{5}$$

where $\dot{\mathbf{p}}_d$ and $\omega_{z,d}$ are the derivatives of the desired position and orientation (along z -axis) of the end effector, respectively. In Eq. (5), the notation \mathbf{J}^\dagger is used to denote the right pseudo-inverse matrix of \mathbf{J} .

Since the manipulator is redundant, the following solution for inverse kinematics has been used:¹³

$$\dot{\mathbf{q}} = \mathbf{J}^\dagger (\dot{\mathbf{e}} + \mathbf{K}\mathbf{e}) + (\mathbf{I} - \mathbf{J}^\dagger \mathbf{J}) \dot{\mathbf{q}}_0, \tag{6}$$

where $\dot{\mathbf{q}}_0$ is an homogeneous solution. For the given manipulator posture, the null space of \mathbf{J} is the subspace of joint velocities that do not produce any end-effector velocity. It is possible to show that this subspace is non-null for a redundant manipulator. In fact, if $\dot{\mathbf{q}}^*$ is a solution for Eq. (3), then the joint velocity vector $\dot{\mathbf{q}} = \dot{\mathbf{q}}^* + (\mathbf{I} - \mathbf{J}^\dagger \mathbf{J}) \dot{\mathbf{q}}_0$ will be a solution for any $\dot{\mathbf{q}}_0$. In this framework, the internal solution will be chosen to deviate from mechanical joint limits.

The task vector \mathbf{e} is defined as

$$\mathbf{e} = \begin{bmatrix} \mathbf{e}_1 \\ \mathbf{e}_1 \end{bmatrix} = \begin{bmatrix} \mathbf{e}_{p,1} \\ \mathbf{e}_{o,1} \\ \mathbf{e}_{p,2} \\ \mathbf{e}_{o,2} \end{bmatrix}, \tag{7}$$

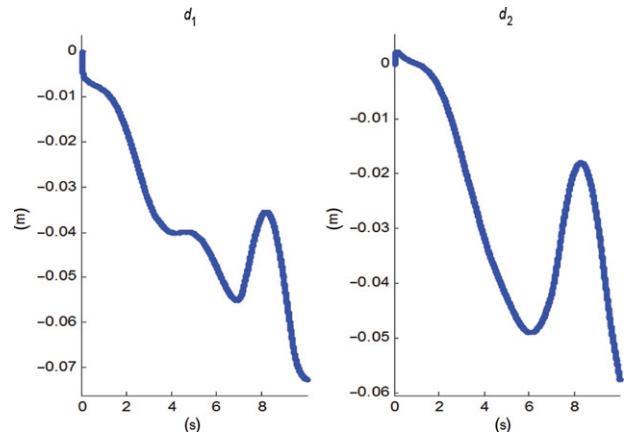


Fig. 7. Desired COM position along sagittal and frontal planes.

where $\mathbf{e}_{p,i}$ and $\mathbf{e}_{o,i}$ denote the position and orientation tasks, respectively, being referred to by subscript i and defined as

$$\begin{aligned} \mathbf{e}_{p,i} &= \mathbf{p}_{d,i} - \mathbf{p}_i, \\ \mathbf{e}_{o,i} &= \eta_i \varepsilon_d - \eta_d \varepsilon_i - \mathbf{S}(\varepsilon_d) \varepsilon_i. \end{aligned} \tag{8}$$

The skew-symmetric matrix \mathbf{S} has been introduced:¹³

$$\mathbf{S}(\varepsilon_d) = \begin{bmatrix} 0 & -\varepsilon_{d,z} & \varepsilon_{d,y} \\ \varepsilon_{d,z} & 0 & -\varepsilon_{d,x} \\ -\varepsilon_{d,y} & \varepsilon_{d,x} & 0 \end{bmatrix}. \tag{9}$$

The orientation error has been calculated based on the unit quaternion,²⁶ defined as $Q = \{\eta, \varepsilon\}$, where

$$\eta = \cos\left(\frac{\theta}{2}\right), \tag{10}$$

$$\varepsilon = \sin\left(\frac{\theta}{2}\right) \mathbf{r}, \tag{11}$$

\mathbf{r} being the unit vector of a rotation axis.

For $i = 1$, the desired position is $\mathbf{x}_{d,1} = \mathbf{0}$ and the desired quaternion is $Q_{d,1} = \{1, \mathbf{0}\}$:

$$\mathbf{e}_{p,1} = \mathbf{p}_l - \mathbf{p}_r, \tag{12}$$

$$\mathbf{e}_{o,1} = -\varepsilon_1, \tag{13}$$

where ε_1 is the vector part of the quaternion related to matrix $\mathbf{R}_r \mathbf{R}_l - \mathbf{I}$, which depends on the matrices giving reference of the end-effector for both arms.

For $i = 2$, the desired position is $\mathbf{x}_{d,2} = \mathbf{p}_d$ and the desired quaternion $Q_{d,2} = \{\eta_d, \varepsilon_d\}$ is defined by the rotation matrix \mathbf{R}_d , which represents rotation along z_0 -axis.

The algorithm presented here has been implemented using Simulink[®]. It has been used to test different situations and some results are presented in Figs. 7–11.

As can be observed, abrupt changes in velocities that characterized our previous work^{2,24} have been solved with the introduction of virtual joints.

It is also clear that the main constraint in a robot (closed-loop chain) has been solved successfully as shown in Fig. 11,

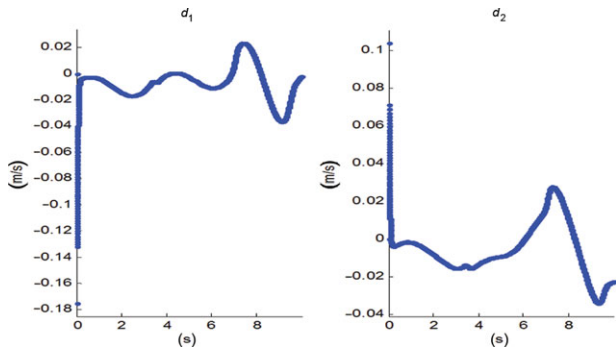


Fig. 8. Desired COM velocity along sagittal and frontal planes.

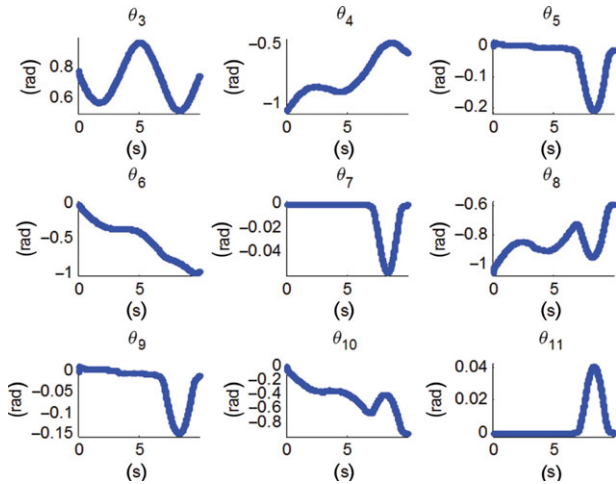


Fig. 9. Joint angles of the arms.

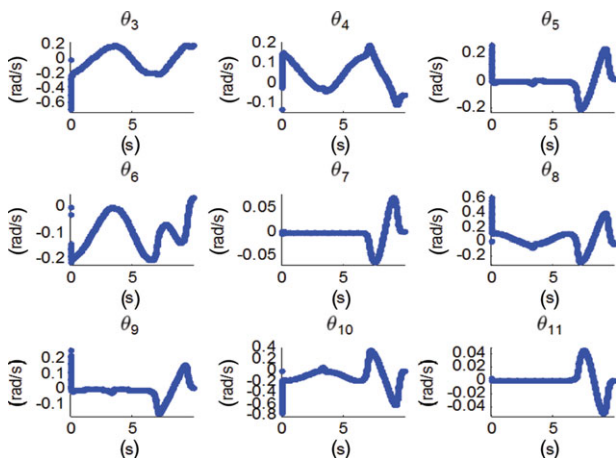


Fig. 10. Joint velocities of the arms.

and that the position and orientation errors with respect to the desired trajectory are negligible.

3.4. Considerations on mechanical structure

From this study, it is clear that 9-DOF would not be sufficient for a whole definition of a trajectory in position and orientation: at least one yaw joint is needed in each arm and a pitch in the trunk.²⁷ Only this way requirements for holding the object and establishing position and orientation of the end-effector could be fulfilled.

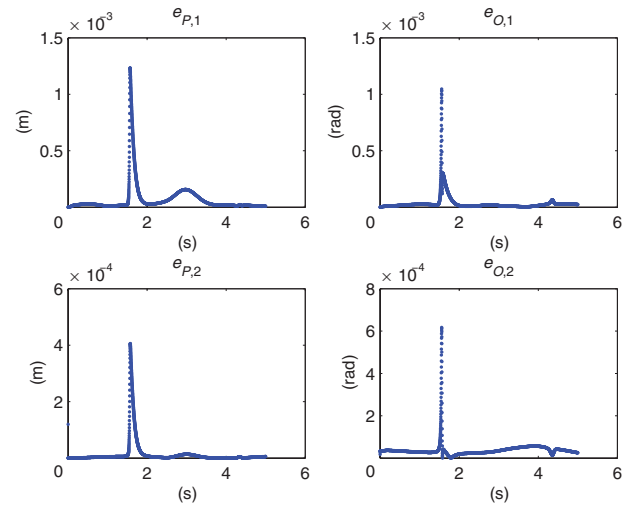


Fig. 11. Position and orientation tasks.

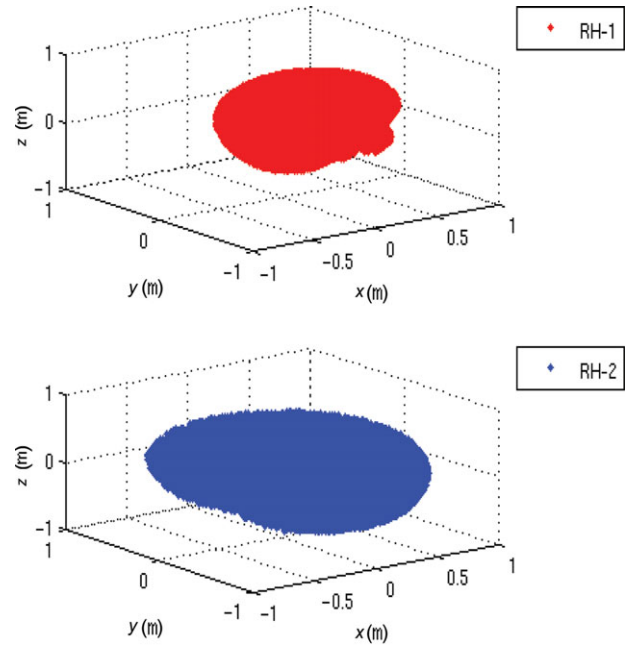


Fig. 12. Comparison between the workspace of RH-1 and RH-2 arms.

This consideration has become an input for the realization of a new RH-2 platform. Moreover, by adding these DOF, increase in the arms workspace is also evident as depicted in Fig. 12.

4. Posture Stability Control

Once the stable patterns required for the task execution are obtained, the following step is to guarantee the stability of the robot pose during the whole task. That is, the COM position demanded by the collaborative control loop must be achieved so that the task can be performed in a stable way. For that purpose, the posture stability control loop is introduced, as will be explained next.

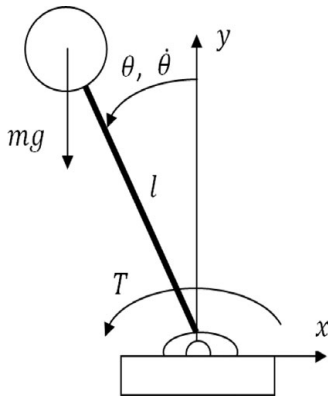


Fig. 13. Single inverted pendulum.

4.1. Model of single inverted pendulum

In a very simplified way, the dynamic model of humanoid robot RH-2 can be considered similar to that of the inverted pendulum given in Fig. 13.

The similarity is established under the following assumptions. The mass of humanoid (m) is concentrated at its COM (tip of the pendulum), which is at a distance l from the floor. The mass of the rigid link is then considered negligible. Besides, the action (torque T) that allows the mass m to move a specific angle θ at speed $\dot{\theta}$ (movement of COM during walking action) is effected by a servomotor (ankle of humanoid robot) fixed at the end of the link (floor). This servomotor performs the control action to ensure stability of the system during the walking action.

It is clear that this model is not complex enough to model the whole dynamics of humanoid robot and to consider its nonlinearities. However, as can be checked in recent literature,^{21,28,29} it gives very good results, even experimentally, as a first approximation. As an improvement to this model, we are currently obtaining first results by modeling RH-2 robot as a double inverted pendulum.^{30,31}

To write the equation of motion of the pendulum,³² let us identify the forces acting on the tip. There is a downward gravitational force equal to mg , where g is the acceleration due to gravity. There is also a frictional force resisting the motion, which we assume to be proportional to the speed of the tip with a friction coefficient k .

Using Newton's second law of motion, we can write the equation of motion in the tangential direction as

$$ml\ddot{\theta} = -mgsin\theta - k\dot{\theta}. \tag{14}$$

Writing the equation of motion in this direction has the advantage that the link tension, which is in the normal direction, does not appear in the equation. In order to obtain a state model for the pendulum, let us take the state variables as $x_1 = \theta$ and $x_2 = \dot{\theta}$. Then, the state equations are

$$\begin{aligned} \dot{x}_1 &= x_2, \\ \dot{x}_2 &= -\frac{g}{l}sinx_1 - \frac{k}{m}x_2. \end{aligned} \tag{15}$$

From the physical description of the pendulum it is clear that it has only two equilibrium positions corresponding to

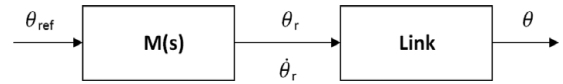


Fig. 14. Posture control system.

the equilibrium points $(0, 0)$ and $(\pi, 0)$. Physically, we can see that these two positions are quite distinct from each other. While the pendulum can indeed rest at the $(0, 0)$ equilibrium point, it can be hardly maintained at the $(\pi, 0)$ point because infinitesimally small disturbance from that equilibrium will take the pendulum away. The difference between the two equilibrium points is in their stability properties.

Another version of the pendulum equations arises if we can apply a torque T to it. This torque is viewed in our case as a control input in equation

$$\begin{aligned} \dot{x}_1 &= x_2, \\ \dot{x}_2 &= -\frac{g}{l}sinx_1 - \frac{k}{m}x_2 + \frac{1}{ml^2}T. \end{aligned} \tag{16}$$

4.2. The COM control problem

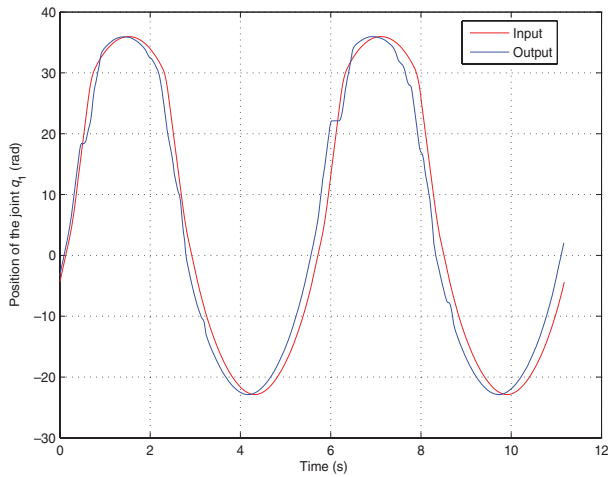
Scheme for the COM control (inverted pendulum) is given in Fig. 14.

The purpose is to control the COM position θ through the action of a servomotor $M(s)$ that gives the appropriate torque at each moment in order to follow the position reference θ_{ref} given by the collaborative control loop (see Fig. 7).

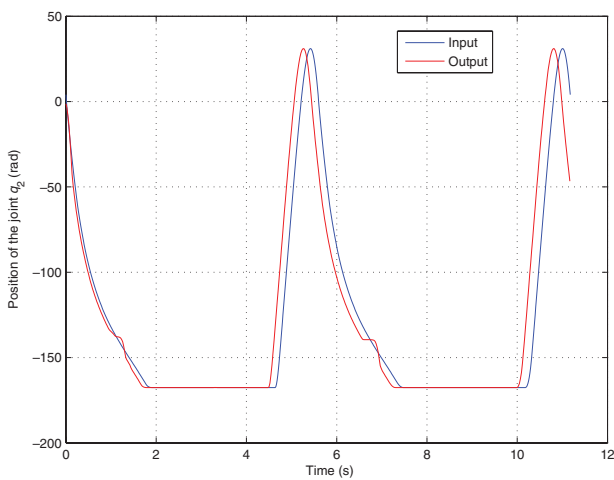
Before introducing this control strategy, it is important to remark the following aspects:

- (1) For our previous prototype of humanoid robot RH-1, the walking action is achieved in an open loop. That is, given the walking patterns for each motor (joint), they follow these patterns in an open loop. This type of control allows RH-1 to walk correctly (take a complete step) in the absence of disturbances, and under the assumption that the motors have been correctly modeled (minor model uncertainties or mismatches). For instance, Fig. 15 shows the walking patterns and the experimental outputs of ankle joints (roll and pitch) involved in a walking action. As observed, robot can take a step in open loop with minor errors²⁴ (see this bibliography reference to check different walking experiments).
- (2) In this work, and as a first approach, we will control in open loop the position of the COM demanded by the collaborative control loop, using the scheme in Fig. 14. For this purpose, we will use an innovative ankle actuator designed for our new prototype RH-2, whose picture is given in Fig. 3. We assume that the experimental ankle + link set is rigid (no joint looseness) and so $(\theta - \theta_r) \rightarrow 0$. Therefore, the experimental transfer function of ankle actuator will be used as a whole (motor+link) reference model for our simulation control scheme. This implies that the dynamics of the link is canceled in this control strategy.

Once this first approach is achieved, the efforts will be devoted to the control of the system in closed loop so that it can be robust to disturbances and model mismatches.



(a) Joint q_1 : right ankle (roll)



(b) Joint q_2 : right ankle (pitch)

Fig. 15. Ankle joints patterns and output positions.

4.3. The COM control strategy

The first step is to obtain the experimental transfer function of the ankle actuator using conventional identification techniques. In our case, it is given by

$$M(s) = \frac{55.03s^2 + 5439s + 2.73 \cdot 10^6}{s^3 + 111.2s^2 + 5.14 \cdot 10^4s + 2.73 \cdot 10^6}. \quad (17)$$

This transfer function is the same for two actuators in the ankle, one in the sagittal plane, and another in the frontal plane (two identical pendulum systems), and will be used as the reference model in our control strategy.

According to the assumptions stated above, the control problem in an open loop must be solved so that the output of the link θ follows the reference θ_{ref} (see Fig. 14). Besides, in our scheme $(\theta_r - \theta_{ref}) \rightarrow 0$, since the motor associated to the link is able to follow the reference with a negligible error. It means that the dynamics of the link is canceled in this strategy. In fact, we are looking for the control action T that allows this fact. To achieve this, the model matching technique³³ is used, based on the input–output linearization of the system. Equations obtained from the application of

this technique are presented next:

$$\begin{bmatrix} \dot{x}_1 \\ \dot{x}_2 \end{bmatrix} = \begin{bmatrix} x_2 \\ -\frac{g}{l} \sin x_1 - \frac{k}{m} x_2 \end{bmatrix} + \begin{bmatrix} 0 \\ \frac{1}{ml^2} \end{bmatrix} u, \quad (18)$$

$$y = x_1.$$

Therefore, the direct relation between the input and output of the system is given by

$$\ddot{y} = -\frac{g}{l} \sin x_1 - \frac{k}{m} x_2 + \frac{1}{ml^2} u, \quad (19)$$

with $u = T$ and $y = \theta$. The purpose is to obtain the control law u so that y follows θ_{ref} as θ_r follows θ_{ref} , that is, a control law so that the whole dynamics matches the model $M(s) = \frac{\theta_r}{\theta_{ref}}$ obtained previously by experimental identification. In order to do so, we define u as

$$u = ml^2 \left[\left(\frac{g}{l} \sin x_1 + \frac{k}{m} x_2 \right) + v \right], \quad (20)$$

so that $\ddot{y} = v$ (from Eq. (19)). Choosing

$$v = \ddot{\theta}_r + a(\theta_r - y), \quad (21)$$

it is obtained that

$$\ddot{y} = \ddot{\theta}_r + a(\theta_r - y). \quad (22)$$

The value of a is selected by trial-error process in order to obtain the minimum tracking error.

Once we have obtained a simulation model that matches the experimental behavior of the motor + link set in open loop, we are currently working on the improvement of the control strategy, closing the loop and addressing robustness issues regarding disturbances and model mismatches (only achievable in closed loop).

4.4. Simulation results

The COM control system described in the previous section has been implemented in Simulink[®] considering the model of the single inverted pendulum applied to robot and the experimental model $M(s)$ of ankle actuator (used as a reference model). The parameters of the system are $m = 50$ kg, $l = 1$ m, $g = 9.8$ m/s², $k = 0.1$, and $a = 0.1$.

We are going to consider the desired COM position from the case study presented in Section 3.3, and shown in Fig. 7. For the compensation in both sagittal and frontal planes, two equal pendulum systems are considered.

The starting equilibrium point is $(\pi, 0)$, which corresponds to a 0 m displacement (l) along the floor plane. We can observe that the COM displacements demanded by the manipulation task are smaller than 7 cm in both planes. Taking into account that the COM is at 1 m from the floor ($l = 1 \sin(\theta)$ from Fig. 13), we can assume that its movements are very constrained to the equilibrium point ($l \simeq \theta$ for $\Delta\theta \simeq 0$ around the upright position), with negligible variations.

Therefore, the inputs to the control system in open loop will be two reference signals of value π (one for each plane). In Fig. 16 the angular position and velocity of the COM for

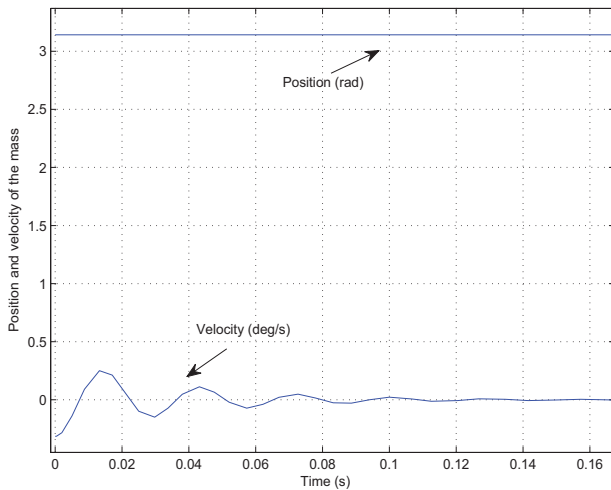


Fig. 16. Angular position and velocity of the tip.

this reference are presented. As can be observed, the control strategy allows the tip to keep in the equilibrium point $(\pi, 0)$.

5. Conclusions and Future Works

A control architecture for human-robot cooperation in collaborative environments has been presented. The different control loops, collaborative and posture ones, have been analyzed and simulated for the case of humanoid robot RH-2.

A closed-chain solution for RH-2 arms supporting an object has been proposed using the powerful instrument of the Jacobian matrix. The posture stability has also been achieved by using the model of the single inverted pendulum and controlling robot's ankle. The case study considered validates the whole control architecture.

A further research will focus on the posture control in closed loop to improve the system's performance. Besides, a study on the addition of new DOF in the robot structure is being carried out in order to improve the manipulation tasks.

Acknowledgments

This work has been supported by the CYCIT Project PI2004-00325 and the European Project Robot@CWE FP6-2005-IST-5, both developed within the research team Robotics Lab in the University Carlos III of Madrid.

References

1. S. A. Green, M. Billingham, X. Chen and J. G. Chase, "Human-robot collaboration: A literature review and augmented reality approach in design," *Int. J. Adv. Robot. Syst.* **5**(1), 1–18 (2008).
2. P. Pierro, C. A. Monje and C. Balaguer, "Modelling and Control of the Humanoid Robot RH-1 for Collaborative Tasks," *Proceedings of IEEE RAS/RSJ Conference on Humanoids Robots*, Daejeon, Korea (2008) pp. 125–131.
3. Y. Yamamoto, H. Eda and X. Yun, "Coordinated Task Execution of a Human and a Mobile Manipulator," *Proceedings of IEEE International Conference on Robotics and Automation*, Vol. 2 (1996), pp. 1006–1011.
4. O. Khatib, L. Sentis, J. Park and J. Warren, "Whole-body dynamic behavior and control of human-like robots," *Int. J. Human. Robot.* **1**, 29–43 (2004).
5. L. Sentis and O. Khatib, "Synthesis of whole-body behaviors through hierarchical control of behavioral primitives," *Int. J. Human. Robot.* **2**(4), 505–518 (2005).
6. P. J. Hinds, T. L. Roberts and H. Jones, "Whose job is it anyway? A study of human-robot interaction in a collaborative task," *Human-Comput. Interact.* **19**, 151–181 (2004).
7. Y. Nakamura and H. Hanafusa, "Optimal redundancy control of robot manipulators," *Int. J. Robot. Res.* **6**(1), 32–42 (1986).
8. M. Gienger, H. Janen and C. Goerick, "Task-Oriented Whole Body Motion for Humanoid Robots," *Proceedings of IEEE International Conference on Humanoid Robots (Humanoids2005)*, Los Angeles, USA (2005) pp. 238–244.
9. N. E. Sian, K. Yokoi, S. Kajita, F. Kanehiro and K. Tanie, "A switching command-based whole-body operation method for humanoid robots," *IEEE/ASME Trans. Mechatron.* **10**(5), 546–559 (2005).
10. O. Khatib, "A unified approach for motion and force control of robot manipulators: The operational space formulation," *Int. J. Robot. Res.* **3**(1), 43–53 (1987).
11. C. Samson, M. Le Borgne and B. Espiau, *Robot Control: the Task Function Approach* (Clarendon Press, Oxford, UK, 1991).
12. B. Siciliano and J.-J. Slotine, "A General Framework for Managing Multiple Tasks in Highly Redundant Robotic Systems," *Proceedings of IEEE International Conference on Advanced Robotics (ICAR'91)*, Pisa, Italy (2003) pp. 1211–1216.
13. B. Siciliano, L. Sciavicco, L. Villani and G. Oriolo, eds., *Robotics: Modelling, Planning and Control* Springer, New York, NY, 2009).
14. S. Kajita and K. Tani, "Study of Dynamic Biped Locomotion on Rugged Terrain," *Proceedings of IEEE International Conference on Robotics and Automation (ICRA)* (1991) pp. 1405–1411.
15. S. Kajita, F. Kanehiro, K. Kaneko, K. Yokoi and H. Hirukawa, "The 3D Linear Inverted Pendulum Mode: A Simple Modeling for a Biped Walking Pattern Generator," *Proceedings of IEEE/RSJ International Conference on Intelligent Robots and Systems (IROS)*, Maui, Hawaii (2001) pp. 239–246.
16. S. Kajita, F. Kanehiro, K. Kaneko, K. Fujiwara, K. Harada, K. Yokoi and H. Hirukawa, "Biped Walking Pattern Generation by Using Preview Control of Zero-Moment Point," *Proceedings of IEEE International Conference on Robotics and Automation (ICRA)*, Taipei, Taiwan (2003) pp. 1620–1626.
17. T. Sugihara and Y. Nakamura, "Variable Impedant Inverted Pendulum Model Control for a Seamless Contact Phase Transition on Humanoid Robot," *Proceedings of IEEE International Conference on Humanoid Robots (Humanoids 2003)*, Germany (2003).
18. R. Altendorfer, U. Saranlı, H. Komsuoglu, D. E. Koditschek, H. Benjamin Brown, M. Buehler, N. Moore, D. McMordie and R. Full, "Evidence for Spring Loaded Inverted Pendulum Running in a Hexapod Robot," In: *Experimental Robotics VII* (D. Rus and S. Singh, eds.) (Springer-Verlag, New York, NY, 2009) pp. 291–302.
19. T. Komura, H. Leung, S. Kudoh and J. Kuffner, "A Feedback Controller for Biped Humanoids that Can Counteract Large Perturbations During Gait," *Proceedings of IEEE International Conference on Robotics and Automation (ICRA)*, Barcelona, Spain, (2005) pp. 2001–2007.
20. T. Komura, A. Nagano, H. Leung and Y. Shinagawa, "Simulating pathological gait using the enhanced linear inverted pendulum model," *IEEE Trans. Biomed. Eng.* **52**(9), 1502–1513 (2005).
21. J. Y. Kim, I. W. Park and J. H. Oh, "Walking control algorithm of biped humanoid robot on uneven and inclined floor," *J. Intell. Robot. Syst.* **48**(4), 457–484 (2007).
22. S. Kajita, M. Morisawa, K. Harada, K. Kaneko, F. Kanehiro, K. Fujiwara and H. Hirukawa, "Biped Walking Pattern Generator Allowing Auxiliary ZMP Control," *Proceedings of IEEE/RSJ International Conference on Intelligent Robots and Systems*, Beijing, China (2006) pp. 2993–2999.

23. V. Fernández, C. Balaguer, D. Blanco and M. A. Salichs, "Active Human-Mobile Manipulator Cooperation Through Intention Recognition," *Proceedings of IEEE International Conference on Robotics and Automation (ICRA'01)*, Seoul, Korea (2001) pp. 2668–2673.
24. C. A. Monje, P. Pierro and C. Balaguer, "Humanoid robot RH-1 for collaborative tasks: A control architecture for human-robot cooperation," *Appl. Bionics Biomech.* **5**(4), 225–234 (2008).
25. Y. Nakamura, H. Hanafusa and T. Yoshikawa, "Task-priority based redundancy control of robot manipulators," *Int. J. Robot. Res.* **6**(2), 3–15 (1987).
26. S. Chiaverini and B. Siciliano, "The unit quaternion: A useful tool for inverse kinematics of robot manipulators," *Syst. Anal. Model. Simul.* **35**, 45–60 (1999).
27. C. Perez, P. Pierro, S. Martínez, L. A. Pabón, M. Arbulú and C. Balaguer, "RH-2: An Upgraded Full-Size Humanoid Platform," *12th International Conference on Climbing and Walking Robots and the Support Technologies for Mobile Machines (CLAWAR'09)*, Istanbul, Turkey (2009).
28. R. P. Kumar, J. W. Yoon and G. S. Kim, "Simplest Dynamic Walking Model with Toed Feet," *Proceedings of IEEE-RAS International Conference on Humanoid Robots*, Daejeon, Korea (2008) pp. 245–250.
29. S. Kajita, T. Nagasaki, K. Yokoi, K. Kaneko and K. Tanie, "Running Pattern Generation for a Humanoid Robot," *Proceedings of IEEE International Conference on Robotics and Automation*, EEUU, Washington DC, (2002) pp. 2755–2761.
30. M. Arbulu, Stable Locomotion of Humanoid Robots Based on Mass Concentrated Model, *Ph.D. Thesis.*, University Carlos III of Madrid, Madrid, Spain.
31. D. Kaynov, Open Motion Control Architecture for Humanoid Robots *Ph.D. Thesis.*, University Carlos III of Madrid, Madrid, Spain.
32. H. K. Khalil, ed., *Nonlinear Systems* (Pearson Education, Upper Saddle River, NJ, 1999).
33. J. A. Isidori, ed., *Nonlinear Control Systems* (Springer-Verlag, London, 1995).